# Self-trapping of low-energy infrared femtosecond beams in lithium niobate

Federico Pettazzi,[1,2] Massimo Alonzo,[1] Marco Centini,[1] Adrian Petris,[3] Valentin I. Vlad,[3] Mathieu Chauvet,[2] and Eugenio Fazio[1]

[1]*Dipartimento di Energetica, Università La Sapienza and CNISM, via A. Scarpa 16, 00161 Roma, Italy*

[2]*Département d'Optique, Institut FEMTO-ST, UMR CNRS 6174, Université de Franche-Comté, 25030 Besançon, France*

[3]*Institute of Atomic Physics, NILPRP-Romanian Center of Excellence in Photonics, Bucharest, Romania*

(Received 29 May 2007; published 20 December 2007)

In this paper we report self-trapping of subnanojoule femtosecond near-infrared beams in photonic-grade undoped bulk lithium niobate under application of an external dc electric field. We show that the phenomenon occurs thanks to the photorefractive effect induced by a weak second-harmonic component generated under large velocity mismatch. It offers a way to extend lithium niobate's photorefractive response to the near-infrared spectrum for peak intensity lower than 1 GW/cm$^2$, which is three orders of magnitude lower than reported in the literature.

DOI: 10.1103/PhysRevA.76.063818 PACS number(s): 42.65.Hw, 42.65.Ky, 42.65.Re

Since its first observation [1], the photorefractive effect has been extensively studied as a useful way to control the propagation of light. During recent years, among many interesting physical phenomena discovered in photorefractive crystals, the formation of spatial solitons has been widely investigated [2–5]. Photorefractive bright solitons are stable in two spatial dimensions, and can be formed using low-power continuous wave beams [5], as well as pulsed illumination in the nanosecond range [6]. Moreover, it was demonstrated that it is possible to observe multimode solitons in these media [7,8], and that a new class of solitons exists based on the propagation of light in discrete lattices [9,10]. In typical investigations performed in photorefractive crystals such as strontium barium niobate, bright spatial solitons are created by focusing a low-power laser beam at the input face of a sample, biased with an electric field applied parallel to the *c* axis. Being related to the photogeneration process, the photorefractive effect is wavelength sensitive and is more efficient at visible wavelengths in ferroelectric crystals [5].

The photovoltaic effect present in lithium niobate (LN) allows the formation of dark spatial solitons [11], but bright spatial solitons can also be obtained in this medium either by using an external electrical bias, larger than the photovoltaic field [12], or by using a background illumination at suitable wavelengths or polarization [13,14]. In congruent photonic-grade undoped LN, the photorefractive effect is due to the presence of vacancies or impurities in the lattice or to the presence of metallic ions in the melt [15]. Impurities with a concentration lower than $10^{16}$ cm$^{-3}$ are sufficient to cause the photorefractive effect.

In the last three years, the propagation of ultrashort near-infrared and infrared pulses in doped and pure LN has also been extensively studied [16–19] because of the potential application in optical processing of information. These investigations have revealed that, when femtosecond pulses propagate in LN, several nonlinear phenomena can be simultaneously present, such as multiphoton absorption and Kerr and photorefractive effects. Studies on the propagation of femtosecond near-infrared light in LN have been performed with energy in the nanojoule regime and peak intensities larger than 1 TW/cm$^2$ [19]. For such intensities the photorefractive effect is driven by multiphoton absorption.

However, in this paper, we report the photorefractive response for a near-infrared femtosecond laser beam with three orders of magnitude lower peak intensity, a regime for which multiphoton processes are negligible. The photorefractive response is induced in spectral regions where the absorption from deep traps is inefficient thanks to quadratic nonlinear processes and in particular to second-harmonic generation. Being linked to the second-harmonic generation and not to higher-order effects such as multiphoton absorption, the photorefractive nonlinearity can consequently be observed at moderate peak intensities. The discovered effect can be exploited to extend photorefractive LN properties to near-infrared wavelengths.

To address this issue we performed experiments of spatial beam modification (self-focusing and -defocusing) using a Ti:sapphire laser, which can operate in both continuous wave (cw) and mode-locking (ML) regimes, delivering an average power of 20 mW at a wavelength of 800 nm. In the pulsed operation regime, the laser delivers 65 fs duration pulses at a repetition rate of 76 MHz. The product between the measured spectral bandwidth and pulse duration is 0.54, larger than the optimum value of the Fourier transform limit of 0.32. When focused to a waist of 12 $\mu$m, as was done in the experiments, these subnanojoule pulses give a maximum peak intensity lower than 1 GW/cm$^2$. The laser beam is linearly polarized along the LN *c* axis and propagates a 6 mm distance in the sample. The photonic grade LN crystal purchased from Crystal Technology has a lithium content of 48.38% and its linear optical absorption is less than 0.0015 cm$^{-1}$ at a wavelength of 1064 nm, as derived from the data sheet [20]. The extraordinarily polarized beam is focused at the input surface of the crystal and light emerging from the sample is collected by a lens and imaged on a charge-coupled device camera in order to study the spatial evolution of the beam at the output of the sample. A frequency-doubled neodymium-doped yttrium aluminum garnet (Nd:YAG) laser illuminates the sample from the side to give a 70 mW/cm$^2$ cw uniform background in order to control the saturation of the photorefractive effect. To obtain a self-focusing effect, a positive external static field of 35 kV/cm is applied in the direction of the *c* axis, as sketched in the setup used by Fazio *et al.* [12].

 

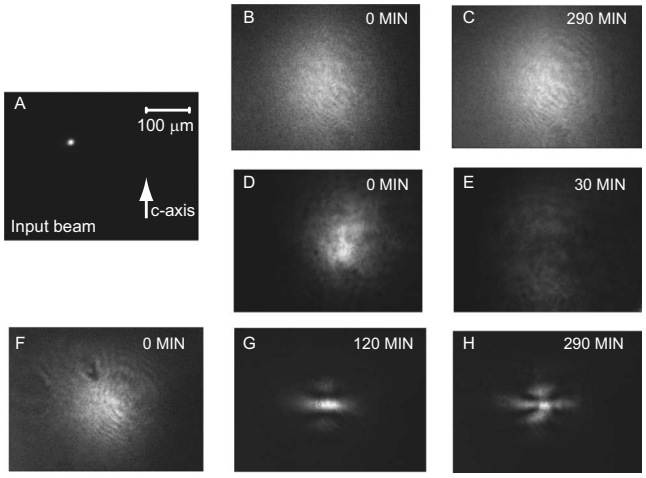


FIG. 1. Experimental results on the propagation of an infrared beam in a 6 mm lithium niobate crystal. Image of the focused beam at the input of the sample (a). Images of the beam in the cw regime at the output face at $t=0$ (b) and 290 min (c) for an applied field of 35 kV/cm. Images of the output face in the ML regime without applied field at $t=0$ (d) and 30 min (e). Images at the output face in the ML regime with an applied field of 35 kV/cm at $t=0$ (f), at 120 (g), and at 290 min (h). A background illumination of 70 mW/cm$^2$ is present and the beam average power is 16 mW.

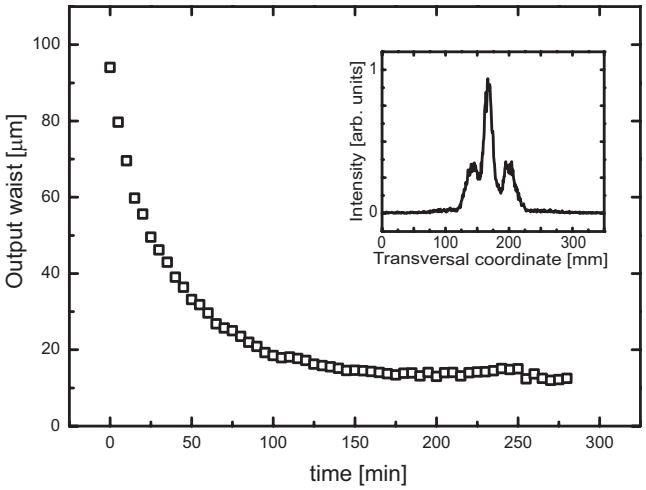


FIG. 2. Dynamic of the self-focusing effect for the infrared beam. The curve is obtained by fitting the central peak of the mode profile along the *c* axis. Inset: profile of the output infrared beam after 250 min.

Results are reported in Figs. 1(a)–1(c) for an experiment performed in the cw regime for an optical power of 16 mW [Fig. 1(a)]. Despite the presence of the external field of 35 kV/cm, no spatial modification of the diffracting output beam is observed after long exposure time [Figs. 1(b) and 1(c)]. This testifies that the beam propagates in the medium in the linear diffraction regime, without experiencing photorefractive index modification. This negligible photorefractive effect is expected at 800 nm in an undoped LN sample. Therefore, the experiment depicted in Figs. 1(a)–1(c) clarifies that, in the range of intensities adopted, the sample is not sensitive at 800 nm cw light and that two-step excitation involving both background and infrared light [21] is not effective as well.

In contrast, focusing light in the ML regime on the crystal input face leads to a remarkably different behavior, as shown in Figs. 1(d) and 1(e). The average beam power impinging on the sample is kept at 16 mW, and in a preliminary experiment the external bias is set to 0. The beam waist at the input face is still 12 $\mu$m, diffracting up to a dimension of 96 $\mu$m at the output face [Fig. 1(d)]. In this femtosecond regime, the peak intensity at the input face of the crystal is thus 0.7 GW/cm$^2$. Over a 30 min exposure time, a nonlinear defocusing effect occurs, which gives the strongly distorted and enlarged output beam in the direction of the *c* axis depicted in Fig. 1(e). We can presume from the slow buildup time of the process that the origin of the process is related to the photorefractive photovoltaic nonlinearity.

As a confirmation of the photorefractive nature of the process, the experiment is repeated with the same parameters as the ones used for Figs. 1(d) and 1(e) except that an external field of 35 kV/cm is applied to the crystal in order to reverse the sign of the nonlinearity. The corresponding experimental observations are reported in Figs. 1(f)–1(h). At the beginning of the experiment the beam diffracts [Fig. 1(f)], but as time evolves, a strong self-focusing effect takes place as reported in Figs. 1(g) and 1(h), taken after, respectively, 125 and 280 min exposure time. The self-focusing effect leads to an output cross-shaped beam consisting in a circular central core surrounded by tails in the directions parallel and orthogonal to the *c* axis. This peculiar output shape is observed consistently in all the experiments involving self-focusing with femtosecond pulses. The reason for this distribution might be related to a nonoptimized refractive index profile for the infrared beam, and is currently under investigation.

In Fig. 2 the width of the central lobe at the output of the sample is reported versus exposure time for the experiment reported in Figs. 1(f)–1(h), showing the dynamic of the self-focusing process and the efficient confinement reached at steady state. In the inset is also shown the output mode profile along the *c* axis taken after 250 min exposure time, with a multihumped mode profile structure clearly visible. The dynamic of the self-focusing process for the central peak is found to follow an exponential decay law, as was previously reported for experiments involving visible light [12]. It constitutes a further indication that the photorefractive effect is the process responsible for the observed spatial beam modification.

It is well known that the photorefractive effect is related to the photogeneration of carriers from deep traps and the associated response time is inversely proportional to the beam average intensity [22]. Since in both cw and ML experiments the average power is kept constant, a question arises as to why carriers are excited in the ML regime but not in the cw regime. In order to elucidate this point, light emerging from the sample is recorded using an optical spectrum analyzer. The measurements reveal that a weak second-harmonic (SH) component is present at the output of the sample as shown in Fig. 3. The SH is found to be extraordinarily polarized and its average power at the output of the

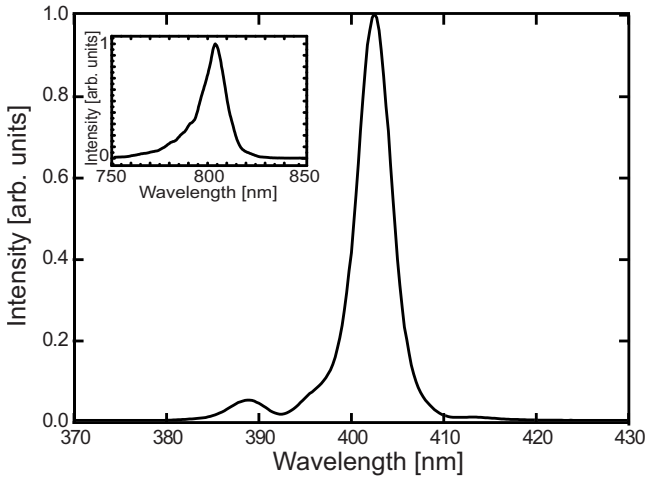


FIG. 3. Measurement of the blue component and of the ir component (inset) of the spectrum at the output of the LN crystal. Average power of launched beam is 20 mW.

sample is evaluated to be 60 nW, a value overestimated because of the difficulty in efficiently eliminating the strong superimposed infrared component. In the inset of Fig. 3 the spectrum of the fundamental harmonic (FH) at the output of the sample is also presented. It is worth noting that this spectrum is identical to the spectrum of the launched pulse, which indicates an insignificant influence of nonlinear effects such as the cascading effect and self-phase-modulation. Moreover, the Kerr coefficient value taken from Ref. [23] ($n_2=1\times10^{-19}$ m$^2$/W), measured in the near infrared in a sample purchased from the same supplier, gives a calculated nonlinear length of 8 cm, which is one order of magnitude larger than our sample length. It thus confirms that the Kerr nonlinear effect is negligible in our experiments.

Let us now analyze the conditions for blue light generation. Although the parametric wave interaction between two extraordinary waves in LN exploits the largest nonlinear coefficient, phase matching is not satisfied for a SH generation (SHG) experiment involving extraordinarily polarized beams at 800 and 400 nm in the bulk crystal. For the lithium niobate crystal used in the present investigation, the nonlinear coefficient involved in such interaction exploits the large coefficient $d_{33}=-33$ pm/V [20]. The very large calculated mismatch $\Delta k=2k_{\mathrm{FH}}-k_{\mathrm{SH}}=-2.5\times10^4$ cm$^{-1}$ corresponds to a coherence length $L_c$ of 2.5 $\mu$m, which is shorter than the pulse length $L_p\approx20$ $\mu$m. Moreover, FH and SH pulses experience temporal walk-off due to group velocity mismatch (GVM). The distance at which the two initially overlapping pulses are separated [24] (the nonstationary length) is $L_{\mathrm{nst}}=27.15$ $\mu$m, which is much shorter than the crystal length.

From these characteristics, it results that the nonlinear interaction corresponds to a strongly phase-mismatched SHG by femtosecond pulses with large GVM [25–27]. The strongly mismatched interaction, together with the large calculated GVM, imply that, at the intensity levels used in the present investigation, cascading effects in the stationary [28] and nonstationary [29] limits are negligible. This is confirmed by the fact that broadening of the FH spectrum at the output of the crystal is not observed in this regime.

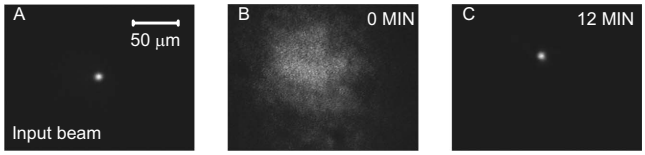


FIG. 4. Self-trapping of 400 nm pulses in pure lithium niobate in the ML regime. Beam at the input face of the crystal (a), and beam at the output face at $t=0$ (b) and 12 min (c). Average optical power is 700 nW, applied field is 35 kV/cm, and background illumination is 70 mW/cm$^2$.

The presence of SH light generated by femtosecond pulses explains the occurrence of the photorefractive effect. When propagating inside the nonlinear medium, the FH generates a SH light whose wavelength is suitable to ionize deep traps present in the forbidden gap. As a result, via the photorefractive effect, without applied field, the photovoltaic effect leads to the beam defocusing [30] shown in Figs. 1(d) and 1(e), while, when an external electric field is applied, the self-focusing effect occurs [31,32], as in Figs. 1(f)–1(h).

To further confirm the key role of SH light in the observed self-focusing, an additional experiment is performed. A 400 nm beam is generated by frequency-doubling the femtosecond 800 nm light in a $\beta$–barium borate crystal. The residual FH is removed using a spectral filter placed before the LN sample. This extraordinarily polarized 700 nW blue beam is then focused at the entrance face of the LN sample to a 9 $\mu$m waist [Fig. 4(a)]. The applied field and background illumination are identical to those in the experiments depicted in Figs. 1(f)–1(h). Experimental observations at the output face of the LN sample are shown in Fig. 4. The 75-$\mu$m-wide initial beam [Fig. 4(b)] self-traps to a minimum waist of 8 $\mu$m in about 12 min [Fig. 4(c)]. Comparison with the results from the initial ML experiment reveals that the response time is commensurate with the inverse of the blue light intensity as predicted by photorefractive theory [22].

By analogy with one-dimensional steady-state spatial soliton theory, we expect that the photorefractive index change induced by the SH beam and sensed by the FH beam is given by the following saturating nonlinearity expression [12,14,33]:

$$\Delta n=-\frac{1}{2}n_e^3 r_{33}\left(E_0\frac{1}{1+I_N}-E_{\mathrm{ph}}\frac{I_N}{1+I_N}\right), \tag{1}$$

where $n_e$ and $r_{33}$ are, respectively, the refractive index and the electro-optic effect coefficient, $E_0$ is the applied electric field, $E_{\mathrm{ph}}$ is the photovoltaic field, $I_N=I_{\mathrm{SH}}/\eta I_B$ with $I_B$ and $I_{\mathrm{SH}}$ respectively, the background intensity and the SH average intensity, and where $\eta=s_B/s_{\mathrm{SH}}$ is the ratio between the background and the SH photoionization cross sections. It thus follows from Eq. (1) that a waveguide is induced when $E_0>E_{\mathrm{ph}}$. Moreover, as was shown previously for photorefractive spatial solitons, the best confinement is obtained in the steady-state regime [34] when $I_N\approx1$. In our experiment, a SH intensity of about 30 mW/cm$^2$ and cross section ratio $\eta$ estimated from LN absorption curves, lead to an $I_N$ value

close to 1 which corroborates the efficiently trapped beam observed in the steady-state regime.

In experiments with femtosecond pulses at 800 nm, two-photon absorption (TPA) could contribute to the photogeneration process. In the present case, the influence of such third-order effect can be ruled out since recently performed measurements in pure LN [16] have confirmed that the TPA contribution to absorption is negligible for femtosecond pulses at 800 nm for intensities below 100 $GW/cm^2$, values which are much higher than the ones used in our experiments.

Instead, SHG, which is a second-order process, is much more efficient. It should be stressed here that SHG acts in the photorefractive mechanism as a TPA-like effect, but the two processes imply very different physical dynamics for free-carrier generation. Indeed, the photorefractive effect is induced by nonlinear absorption of the infrared beam for TPA, while in the present case it is given by linear absorption for the SH beam.

In conclusion, in this paper results on the photorefractive effect indirectly stimulated by a low-intensity near-infrared femtosecond pulse in a nominally undoped lithium niobate sample are reported. The application of an external bias induces a self-focusing effect that traps the beam. We show that the observed trapping is induced by a weak second-harmonic beam generated during propagation of the infrared pulses in the sample. These results offer a way to extend in the near-infrared spectrum the photorefractive response of photorefractive quadratic crystals such as LN by use of the quadratic nonlinear effect without need for phase matching or high peak power. For instance, the photorefractive response of LN could potentially be extended up to telecommunication wavelengths.

Financial support from Università Italo-Francese (UIF-UFI) through the VINCI program, from Italian Project PRIN "Amplificatori e sorgenti laser integrati in guide solitoniche in Er:$LiNbO_3$," from Romanian Project No. CEx05-D11-26/05.10.2005, and from the Collaboration Agreement in R&D between Italy and Romania (Project No. 18) is gratefully acknowledged. We also acknowledge valuable discussions with A. Belardini and O. Bouganov.

[1] A. Askin, G. D. Boyd, J. M. Dziedzic, R. G. Smith, A. A. Ballman, J. J. Levinstein, and K. Nassau, Appl. Phys. Lett. **9**, 72 (1966).
[2] M. Segev, G. C. Valley, B. Crosignani, P. Di Porto, and A. Yariv, Phys. Rev. Lett. **73**, 3211 (1994).
[3] M. Segev, M. Shih, and G. C. Valley, J. Opt. Soc. Am. B **13**, 706 (1996).
[4] K. Kos, H. Meng, G. Salamo, M. F. Shih, M. Segev, and G. C. Valley, Phys. Rev. E **53**, R4330 (1996).
[5] M. F. Shih, M. Segev, G. C. Valley, G. Salamo, B. Crosignani, and P. Di Porto, Electron. Lett. **31**, 862 (1995).
[6] K. Kos, G. Salamo, and M. Segev, Opt. Lett. **23**, 1001 (1998).
[7] M. Mitchell, M. Segev, and D. N. Christodoulides, Phys. Rev. Lett. **80**, 4657 (1998).
[8] T. Carmon, C. Anastassiou, S. Lan, D. Kip, Z. H. Musslimani, M. Segev, and D. Christodoulides, Opt. Lett. **25**, 1113 (2000).
[9] D. Neshev, E. Ostrovskaya, Y. Kivshar, and W. Krolikowski, Opt. Lett. **28**, 710 (2003).
[10] J. W. Fleischer, T. Carmon, M. Segev, N. K. Efremidis, and D. N. Christodoulides, Phys. Rev. Lett. **90**, 023902 (2003).
[11] M. Taya, M. C. Bashaw, M. M. Fejer, M. Segev, and G. C. Valley, Phys. Rev. A **52**, 3095 (1995).
[12] E. Fazio, F. Renzi, R. Rinaldi, M. Bertolotti, M. Chauvet, W. Ramadan, A. Petris, and V. I. Vlad, Appl. Phys. Lett. **85**, 2193 (2004).
[13] C. Anastassiou, M. Shih, M. Mitchell, Z. Chen, and M. Segev, Opt. Lett. **23**, 924 (1998).
[14] W.-L.-She, C.-C. Xu, B. Guo, and W. K. Lee, J. Opt. Soc. Am. B **23**, 2122 (2006).
[15] W. Yan, Y. Kong, L. Shi, L. Sun, H. Liu, X. Li, D. Zhao, J. Xu, S. Chen, L. Zhang, Z. Huang, S. Liu, and G. Zhang, Adv. At., Mol., Opt. Phys. **45**, 2453 (2006).
[16] O. Beyer, D. Maxein, K. Buse, B. Sturman, H. T. Hsieh, and D. Psaltis, Opt. Lett. **30**, 1366 (2005).
[17] O. Beyer, I. Breunig, F. Kalkrum, and K. Buse, Appl. Phys. Lett. **88**, 051120 (2006).
[18] V. I. Vlad, A. Petris, A. Bosco, and E. Fazio, J. Opt. A, Pure Appl. Opt. **8**, S477 (2006).
[19] S. Juodkazis, M. Sudzius, V. Mizeikis, H. Misawa, E. G. Gamaly, Y. Liu, and O. A. Lochev, Appl. Phys. Lett. **89**, 062903 (2006).
[20] http://www.crystaltechnology.com/docs/LNopt.pdf
[21] C. Hou, Y. Pei, Z. Zhou, and X. Sun, Phys. Rev. A **71**, 053817 (2005).
[22] N. Fressengeas, D. Wolfersberger, J. Maufoy, and G. Kugel, Opt. Commun. **145**, 393 (1998).
[23] R. DeSalvo, A. A. Said, D. J. Hagan, E. W. Van Stryland, and M. Sheik-Bahae, IEEE J. Quantum Electron. **32**, 1324 (1996).
[24] S. M. Saltiel, K. Koynov, B. Agate, and W. Sibbett, J. Opt. Soc. Am. B **21**, 591 (2004).
[25] R. Malek Rassoul, A. Ivanov, E. Freysz, A. Ducasse, and F. Hache, Opt. Lett. **22**, 268 (1997).
[26] M. Mlejnek, E. M. Wright, J. V. Moloney, and N. Bloembergen, Phys. Rev. Lett. **83**, 2934 (1999).
[27] W. Su, L. Qian, H. Luo, X. Fu, H. Zhu, T. Wang, K. Beckwitt, Y. Chen, and F. Wise, J. Opt. Soc. Am. B **23**, 51 (2006).
[28] M. L. Sundheimer, Ch. Bosshard, E. W. Van Stryland, G. I. Stegeman, and J. D. Bierlein, Opt. Lett. **18**, 1397 (1993).
[29] F. O. Ilday, K. Beckwitt, Y-F. Chen, H. Lim, and F-W. Wise, J. Opt. Soc. Am. B **21**, 376 (2004).
[30] S. Orlov, A. Yariv, and M. Segev, Appl. Phys. Lett. **68**, 1610 (1996).
[31] S. Lan, M. Shih, G. Mizell, J. A. Giordmaine, Z. Chen, C. Anastassiou, and M. Segev, Opt. Lett. **24**, 1145 (1999).
[32] F. Pettazzi, V. Coda, M. Chauvet, and E. Fazio, Opt. Commun. **272**, 238 (2007).
[33] A. D. Boardman, W. Ileki, and Y. Liu, J. Opt. Soc. Am. B **19**, 832 (2002).
[34] D. N. Christodoulides and M. I. Carvalho, J. Opt. Soc. Am. B **12**, 1628 (1995).